J Mater Sci (2007) 42:7381–7388
DOI 10.1007/s10853-007-1596-8

Silica coating of vapor grown carbon fibers

Huma R. Jafry · Elizabeth Whitsitt · Andrew R. Barron

Received: 28 November 2006 / Accepted: 8 February 2007 / Published online: 15 May 2007

Abstract Silica coatings have been applied to vapor grown carbon fibers (VGCFs) by a liquid phase deposition process. Unlike the coating of single walled carbon nanotubes, the addition of a surfactant to ''solubilize'' the VGCFs results in an extremely non-uniform coating consisting of spherical silica aggregated around the tubes. As was observed for fullerenes, hydroxylation of the surface of the VGCF appears to be key to the formation of a uniform silica coating. Irrespective of the type of VGCF, heating a suspension of VGCFs in nitric acid to dryness (Type II) gave us the best results in terms of silica growth around the VGCF and there is a correlation between the percent of hydroxyls present on the VGCF surface and on the type of growth that occurs on the VGCF. Nitric acid treatment of VGCFs for 1 day in solution were precipitated with acetone (Type III treatment), and then coated with silica. This acid treatment made the coated fibers highly soluble in EtOH.

Introduction

Vapor grown carbon fibers (VGCFs) have been known since the late 19th century [1], and much of the subsequent research has been concerned with understanding the growth mechanism and properties. The primary use of VGCFs has been in composites due their high strength, stiffness, and resistance to corrosion at high temperatures, while recent applications include their use as anode materials and in hydrogen storage [2]. The VGCFs are produced when very small particles (~10 nm) of a transition metal catalyst (e.g., iron) are heated with a hydrocarbon (e.g., methane or benzene) and hydrogen. At temperatures above 900 °C, the catalyst particles grow long and slender filaments of mostly graphitic carbon [3, 4]. X-ray diffraction studies have shown that the fibers are made of concentric cylinders of graphitic basal planes [5]. In addition, VGCFs have a higher graphitic perfection than the pitch or PAN fibers produced at comparable temperatures. In order to control the interaction between VGCFs and a composite matrix, it has generally been accepted that surface treatment of carbon fibers is important to promote better adhesion and dispersion within the matrix [6].

Standard space shuttle tiles (LI-2200) are made of silica fibers that have a density of approximately 3.52 kg m^{-3} and low thermal conductivity (thru-the thickness) of 7.443×10^{-2} W m^{-1} K^{-1}at low temperatures [7]. The ceramic fibers are made by combining constituent silica fibers into a water-based slurry, which is then axially compressed in a casting tower and fired in a high temperature furnace. The result is a three dimensional, highly complex, anisotropic fiber that is aligned normal to the pressing direction [8]. The silica fibers are then combined in an amorphous assembly of fibers held together with a colloidal silica binder. The diameter of the silica fiber is approximately 10 μm, and the overall porosity of the tile is close to 90% [9]. It is generally assumed that the pore size between fibers is three times the diameter of the fibers. The high porosity helps keep the thermal conductivity down at lower temperatures. However, at temperatures above 1,093 °C radiative transfer of heat occurs that is directly

H. R. Jafry · E. Whitsitt · A. R. Barron (✉)
Department of Chemistry, Department of Mechanical Engineering and Materials Science, and Richard E. Smalley Institute for Nanoscale Science and Technology, Rice University, Houston, TX 77005, USA
e-mail: arb@rice.edu
URL: www.rice.edu/barron

proportional to the pore size of the ceramic material used since the pores are transparent to radiation [10]. The photons go through the pores and are absorbed and reradiated by the fibers. In order for the space shuttle tiles to stay thermally insulating at higher temperatures, the porosity of the ceramic tile could to be reduced by closing the pores of the material through which the radiative heat transfer can take place. This could be achieved by adding more silica fibers which would lead to an undersirable increase in tile density, and more significantly the ceramic forms a conductive path through the solid phase specially at lower temperatures. Thus, filling the pores with silica fibers increases conduction heat at low temperatures and not doing so creates radiation heat at high temperatures [11].

Our hypothesis is that filling the pores with nanoscale carbon fibers coated with silica will allow for a greater surface area for absorption and reradiation of photons, without affecting the density of the silica tile significantly. We have previously demonstrated that single walled carbon nanotubes (SWNTs) can be coated with silica, thus creating nanoscale silica fibers [12]. Unfortunately at present the use of silica coated SWNTs would not be economically advantagous since the pore size is large. However, it would be cost effective to use VGCFs as a template. Our goal is therefore to develop smooth and even silica coating on VGCFs. These silica coated VGCFs (SiO_2-VGCFs) could then be employed in composite applications and as silica fiber templates.

We have previously demonstrated that in order to prepare SWNTs with a uniform contiguous coating of silica, a liquid phase deposition (LPD) process [13, 14] should be employed in place of sol–gel. In addition, cationic surfactants such as dodecyl trimethylammonium bromide (DTAB) are required to disperse SWNTs in aqueous solutions for subsequent coating using a fluorosilicic acid/fumed silica solution [12], alternatively, coating under basic conditions required the use of anionic surfactants [15]. In the absence of a surfactant, agglomerates of silica are formed instead of coatings. A similar result was observed for fullerenes where hydroxyl substituents are required to provide nucleation sites [16]. In a similar manner hydroxyl groups were necessary to obtain uniform $CaCO_3$ coatings on SWNTs [17]. Thus, we have investigated the use of both a surfactant and surface activation prior to coating as a means of ensuring uniform coating of VGCFs.

Experimental

Materials used

Vapor grown carbon fibers were obtained from Wright Patterson Air Force Base (Pyrograph III, 450.19, Applied Science Inc), NASA Johnson Space Center (Pyrograph III, 513.08, Applied Science Inc.) and MER Corporation (MRCSD). Fluorosilicic acid (34% by weight, H_2SiF_6) and fumed silica (99% pure, SiO_2) were obtained commercially (Sigma–Aldrich) and were used without any further purification. Surfactants dodecyl tri-methyl ammonium bromide (DTAB) were used as received (Sigma–Aldrich). Nitric acid (69–71 wt.%), MeOH and acetone (Fisher), and EtOH (absolute 200 proof, Aaper) were used as received. Ultra pure (UP) water was obtained from a Millipore Milli-Q UV water filtration system. Solutions were filtered using Millipore Express PLUS Membranes made of polyethersulfone with 0.22 and 0.1 μm pore sizes and Cole Parmer PTFE filters with 0.20 μm pore size. All reactions were performed in polypropylene centrifuge tubes (50 mL, Corning) in a heated water bath. Centrifugation was performed on an IEC Centra MP4 centrifuge.

Nitric acid oxidation

Three different oxidation methods are employed to pretreat the VGCFs in order to promote coating of silica. Type I treatment was performed at NASA Johnson Space Center from whom we received the treated VGCFs. Type II treatment of VGCFs is the same treatment that was performed on VGCFs in our lab previously [18]. Type III treatment is similar to previously published oxidation treatments where VGCFs are refluxed in concentrated nitric acid (69–71 wt.%) at 115 °C for different time intervals [4].

Type I treatment performed on the VGCFs by NASA Johnson Space Center was achieved by refluxing VGCFs (~1 g) in concentrated nitric acid (27 wt.%, 200 mL) in a round bottom flask for 2 days. After which the solution was cooled to room temperature and continually stirred for 5 days. The treated VGCFs were filtered and washed with DI water until a pH 6 was achieved. The fibers were washed with anhydrous EtOH and dried in open air at room temperature.

Type II acid treatment was achieved by reacting VGCFs (~50 mg) in concentrated nitric acid (50–70 wt.%, 50 mL). The solution was stirred in an open Pyrex beaker at 40 °C continuously for 5 days. The nitric acid evaporated and the oxidized VGCFs left were scraped off the bottom and collected [18].

Type III acid treatment involves refluxing VGCFs (~250 mg) in concentrated nitric acid (50–70 wt.%, 250 mL) for 1 day in a round bottom flask. The solution was allowed to cool to room temperature and was added slowly to DI water (375 mL). The mixture was allowed to cool for 20 min. At small intervals, acetone (500 mL) was added to this mixture, and the solution was vacuum filtered using a 0.2 μm Teflon filter. The filtrate was dried in a

Table 1 Atomic concentration of C_{1s} and O_{1s} obtained from XPS

VGF sample ID	Treatment	C_{1s} (%)	O_{1s} (%)
Pyrograph III (NASA)	n/a	95.59	4.41
Pyrograph III (NASA)	Type I	95.37	4.63
Pyrograph III (NASA)	Type II	90.25	9.75
Pyrograph III (Air Force)	n/a	94.9	5.1
Pyrograph III (Air Force)	Type II	72.63	27.37
Pyrograph III (Air Force)	Type III	79.59	20.41
MER corp.	n/a	99.23	0.77
MER corp.	Type I	97.23	2.77
MER corp.	Type II	96.18	3.82

beaker at 40 °C. Table 1 summarizes the relative increase in oxygen content of the VGCFs before and after the different acid treatments as determined by XPS.

Silica coating

Two silica-coating treatments are employed: with and without surfactant. Fumed silica (3 g) was added to fluorosilicic acid (H_2SiF_6, 50 mL, 3.20 M) in a Teflon cup and the mixture was stirred overnight. The concentrated solution was filtered through a 0.22 μm Millipore filter. Pretreated VGCFs (25 mg) were added to DI water (100 mL) in a glass beaker, bath sonicated for 20 min, and then heated overnight at 85 °C. The VGCF/water mixture (17.2 mL) was added to the concentrated H_2SiF_6 solution (7.8 mL) in a plastic centrifuge tube and placed in a water bath at 40 °C. The addition of water diluted the H_2SiF_6 solution to 1.0 M. The solutions were allowed to react for 4, 8, 20, and 24 h. The reaction was then centrifuged at 4,400 rpm for 15 min and the supernatant was discarded. The remaining solid was dispersed in a MeOH:EtOH (1:4) solution. The centrifugation/dispersion cycle was repeated four times.

Vapor grown carbon fibers (25 mg) previously treated in nitric acid air for 5 days (Type II acid treatment) were mixed in DI water (100 mL), bath sonicated for 20 min, and heated overnight at 85 °C. DTAB (1% by wt., 1 g) was added to the VGCF/water solution and pulse sonicated (3 s on/1 s off) in a probe sonicator for 20 min. VGCF/water mixture (17.2 mL) was added to the concentrated H_2SiF_6 solution (7.8 mL) in a plastic centrifuge tube and a stirrer placed in a water bath at 40 °C. The solutions were allowed to react for 4, 8, 20, and 24 h. The reaction was then centrifuged at 4,400 rpm for 15 min and the supernatant was discarded. The remaining solid was dispersed in a MeOH:EtOH (1:4) solution. The centrifugation/dispersion cycle was repeated four times. Table 2 summarizes the appearance of the silica coatings with different acid pretreatment, deposition times, and the effect of surfactant.

Characterization

Characterization was performed using a FEI XL30 Schottky field-emission environmental scanning electron microscope (ESEM) with energy dispersive X-ray spectroscopy (EDX) capability and a JEOL 6500F thermal field-emission scanning electron microscope; FEI Quanta 400 field-emission ESEM with dispersive spectroscopy capability, a JEOL 6500F thermal field-emission scanning electron microscope and a backscatter detection capability was also used for characterization. These were used at accelerating voltages of 30 and 15 kV, respectively. Samples were mounted with carbon tape onto aluminum microscopy specimen mounts (Electron Microscopy Sciences).

XPS analysis was performed on samples pressed on an indium foil (99.999% Sigma–Aldrich). Surveys as well as high-resolution spectra were acquired using a PHI Quantera X-ray photoelectron microscope instrument equipped with an AlK_α monochromatized source with 100.3 W and 25 kV. Survey spectra were acquired using a pass energy of 140 eV with 0.5 eV/step and for the high-resolution spectra a pass energy of 26 eV with a 0.1 eV/step were used. The surveys were acquired for 3 min and the high-resolution spectra were scanned for 10 h. An electron beam of 30 μA was used to compensate for the charging. PC-COMPASS 7.1 software was used to acquire the data and Multipak 7.0.1 program was used for data processing. All the spectra were corrected for charging by using as an internal reference the O 1s peak settled at 531.00 eV.

Raman spectroscopy on solids (785 nm excitation) was performed using a Renishaw Raman microscope. Samples were mounted on double stick tape. Attenuated total reflectance infrared spectroscopy (ATR-IR, 4,000–600 cm^{-1}) of solids was obtained using a Nicolet Nexus 670 FT-IR with a diamond window.

Results and discussion

We have previously reported that the LPD of silica from fluorosilicic acid/fumed silica solutions yield silica coatings containing fluorine [19]. The coatings on the VGCFs contain similar levels of fluorine as indicated by IR and Raman spectroscopy (Figs. 1 and 2). In addition, the Raman spectrum (Fig. 2) shows the presence of VGCFs within the silica coating.

If no acid pretreatment is employed then the VGCFs show little or no coating. Instead they appear to be incorporated into particulate silica (Fig. 3). We have obtained similar results with the LPD of silica in the presence of C_{60} [18]. The most uniform coatings were obtained with the Type II acid treatment (see Experimental). Figure 4a shows

Table 2 Summary of coating experiments

VGCFs	Acid treatment	Surfactant	Deposition time (h)	Appearance
Pyrograph III (NASA)	I	None	4	Thick overlapping colloidal growth along the VGCFs
Pyrograph III (NASA)	I	None	20	Colloidal growth on agglomerated VGCFs
Pyrograph III (NASA)	I	None	24	Thin coating, sparse colloids
Pyrograph III (NASA)	II	None	4	Thin and even growth; regions of thicker growth
Pyrograph III (NASA)	II	None	8	Thicker growth than 4 h; uniform growth with few very small colloids
Pyrograph III (NASA)	II	None	20	Sparse but bigger colloids along the VGCFs
Pyrograph III (NASA)	II	None	24	Thick tightly packed colloids
Pyrograph III (Air Force)	II	None	4	Uniform coating, few scattered colloids
Pyrograph III (Air Force)	II	None	8	Uniform coating, with colloids
Pyrograph III (Air Force)	II	None	20	Some uniform coating; significant colloids
Pyrograph III (Air Force)	II	None	24	Mostly colloids, chunky covering VGCFs
Pyrograph III (Air Force)	II	DTAB	4	Evenly spaced colloids along the VGCFs
Pyrograph III (Air Force)	II	DTAB	8	Evenly spaced colloids along the VGCFs
Pyrograph III (Air Force)	II	DTAB	20	Colloidal growth; colloids growing on top of one another
Pyrograph III (Air Force)	II	DTAB	24	Colloidal growth; colloids growing on top of one another
Pyrograph III (Air Force)	III	None	0.5	
Pyrograph III (Air Force)	III	None	3	VGCFs in a silica matrix
MER	I	None	4	Even and thick silica growth; some sparsely spaced colloids
MER corp.	I	None	8	Some fibers have thick uniform growth; colloids and thick silica growth
MER corp.	I	None	20	Mostly colloidal growth
MER corp.	I	None	24	Heavy colloidal growth; chunks of silica between or binding VGCFs
MER corp.	II	None	4	Even, thin growth
MER corp.	II	None	8	Even and silica growth; sparse small colloids
MER corp.	II	None	20	Even and thick growth; colloids and thick growth
MER corp.	II	None	24	Thicker and more colloids than the 20 h. run; colloids along VGCFs

an SEM image of the silica-coated VGCFs. As may be seen under optimum conditions each VGCF appears uniformly coated with an essentially featureless coating. EDX analysis showed that each of the VGCFs was coated with silica. Based upon a comparison with the untreated VGCFs (Fig. 5a) the coating is approximately 90–100 nm thick after 4 h treatment (Fig. 5b). In order to compare the conformality of the silica coatings in comparison to that previously reported for SWNTs [16] the use of DTAB surfactant was investigated.

Adding surfactant to the VGCF/H_2O solution and then exposing the suspension to the LPD solution gave a very uneven and colloidal growth on the tubes (Fig. 6). Previously in our lab, it has been demonstrated that adding DTAB to the LPD silica solution creates individual spheres as a result of the micelles in solution [20]. The presence of surfactant on the VGCF reaction appears to have had the same templating effect and encourages growth of silica spheres. It is interesting to note that the majority of the spheres are attached to the sidewalls of the VGCFs and that

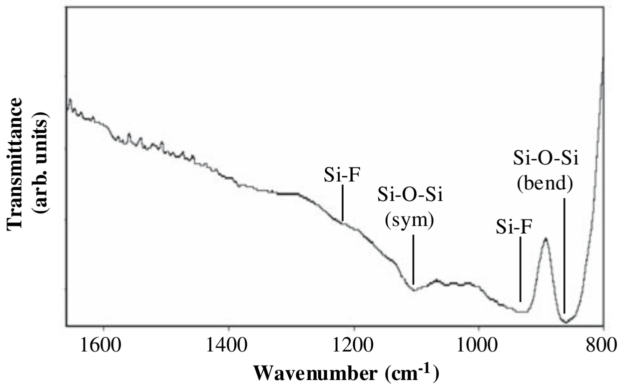

Fig. 1 IR spectra showing the presence of Si–O–Si present around the VGCFs

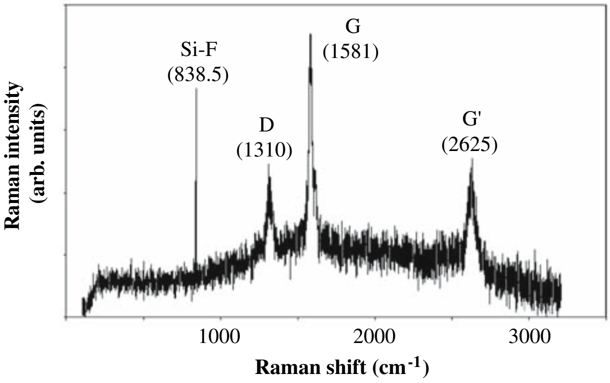

Fig. 2 Raman spectra (using 532 nm excitation) of silica coated VGCFs showing the presence of VGCFs and the F-containing silica. Band assignments are provided

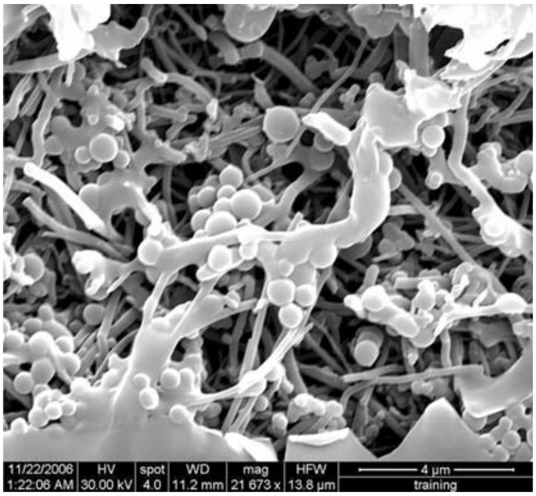

Fig. 3 SEM image of Type II treated VGCFs (Pyrograph III) treated with silica LPD solution without any acid pretreatment of the VGCFs showing the presence of uncoated VGCFs and silica particles

there does appear to be a coating on the fibers under the spheres. We propose that the presence of the DTAB results in a competition between deposition on the VGCF surface and the micelle. We can conclude that, in contrast to our results with SWNTs, we have found that in the case of VGCFs, acid treatment rather than a surfactant promotes uniform coatings.

Effect of VGCF pretreatment

Amongst the three different acid treatments that have been performed on the VGCFs, the Type II method developed in our laboratory (involving heating VGCFs in nitric acid in open air for 5 days) gave the best coating for the VGCFs irrespective of their manufacturer's source (Table 2).

The Type I treatment developed by NASA Johnson Space Center gave a comparable silica coating for fibers treated from MER Corp., but gave worse results for Pyrograph III VGCFs that were obtained from NASA. In general acid treatment Type I resulted in lumpy coatings, although all the VGCFs appeared coated (Fig. 7). In contrast, Type III treatment resulted in the VGCFs becoming imbedded in large silica particles (Fig. 8). In addition, SEM characterization was difficult to perform on tubes oxidized using Type III acid treatment, because after coating with silica the tubes are still highly dispersible in MeOH:EtOH (1:4) solution making it difficult to centrifuge them. These coated fibers would be ideal for applications in which silica-VGCFs are required to stay suspended in solution for to allow for further surface modification, i.e., reaction with an organic silane to promote miscibility in organic matrices (e.g., visco-elastic surfactants or fracturing fluids).

As we noted in the introduction, we have observed that LPD growth onto carbon nanomaterials requires surface activation of the material in order to ensure uniform deposition [18, 19]. In the case of silica LPD it has been reported that it is important for the surface of the substrate to have hydroxyl groups [21]. The reaction shown in Eq. 1 is an oversimplified model of the overall LPD silica growth.

$$H_2SiF_6 + 2H_2O \rightarrow SiO_2 + 6HF$$

However, during this reaction it is proposed [23] that silicon-halide species are also formed, which is hydrolyzed to form $SiF_n(OH)_{4-n}$ ($n < 4$) in supersaturated H_2SiF_6 solution. The siloxane oligomers are then adsorbed onto the surface of the substrate where condensation occurs resulting in bonding with the hydroxyl groups on the surface [22]. In the absence of surface hydroxides, homogeneous nucleation occurs resulting in a particulate material rather than a coating. It would be expected therefore that the

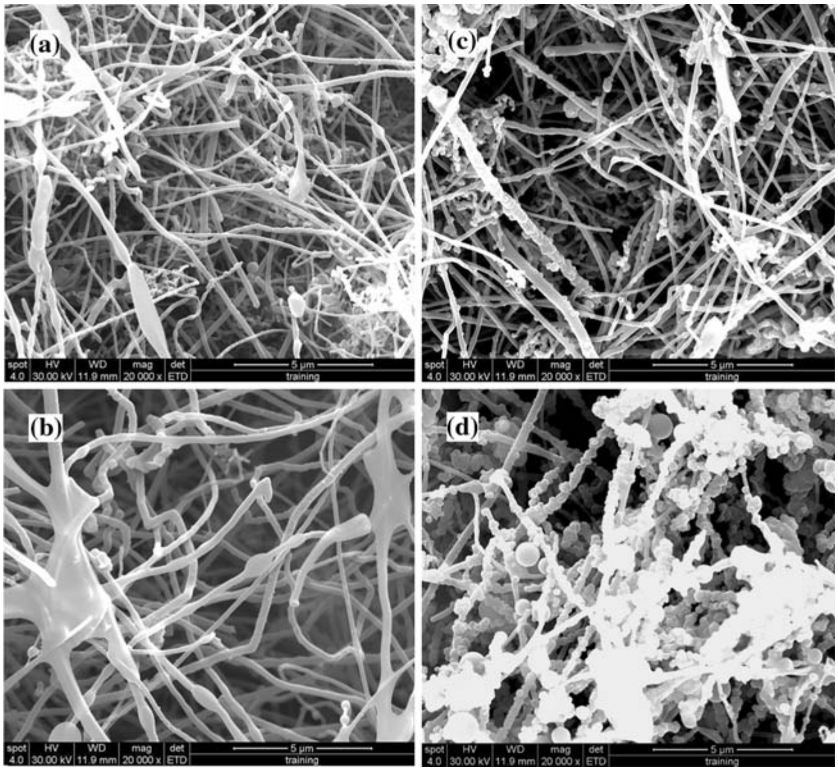

Fig. 4 SEM image of Type II treated VGCFs (Pyrograph III) coated with silica for (**a**) 4 h, (**b**) 8 h, (**c**) 20 h, and (**d**) 24 h

greater the hydroxylation of the VGCFs the greater the propensity for the formation of a contiguous coating. XPS results in Table 1 show that compared to all the different raw tubes as received. There is an increase in oxidation for each acid treatment. It has been reported [4, 23, 24] that the C_{1s} spectra can be fitted for different carbon types (i.e., graphitic, C–O, C=O, and carbonate), e.g., Fig. 9. The Table 3 provides the relative hydroxyl content (as assigned to a peak at 286.0–286.9 eV) for each of the acid treated VGCFs.

Irrespective of VGCF source, Type I treatment results in the smallest increase in oxygen (and hydroxyl) content as compared to the untreated samples (see Tables 1 and 3). This is reflected in the non-uniform silica growth shown in Fig. 7, where there is significant colloid formation. In contrast, silica growth on tubes with a higher percentage of hydroxyl groups shown in Fig. 4 shows a much more uniform and continuous coating. The colloidal growth is most likely because presence of hydroxyl groups allow for a heterogeneous growth of silica on surface, while a homogenous colloidal silica growth is seen when few or no hydroxyls are present [16].

Also consistent with the quality of the observed coating and the oxygen content is that the Type II treatment has significantly greater oxygen content than the VGCFs treated with the Type I treatment (Tables 1 and 3). Type III acid treatment is comparable to Type II treatment in terms of percent oxidation and percent hydroxyl groups present suggesting the coating results should be comparable. However, for reasons not completely understood, the Type III solution is difficult to centrifuge in the presence of alcohols compared to tubes treated with Type II oxidation. The only significant difference between the VGCFs exposed to Type II and III treatments is that XPS suggest the latter contain a higher percentage of carbonyl, quinine, and carboxyl (i.e., C=O) groups.

Effect of deposition time

The deposition time plays a very crucial role in growth of silica around the VGCFs. Comparing the 4-h runs to the 8, 20 and 24 h runs in Fig. 4, one can easily tell of the excessive colloidal growth on the fibers (Table 2). One reason for this could be that heterogeneous silica growth occurs on the surface of the substrate due to the presence of the hydroxyl groups. However, once the silica film is formed around the tube, additional silica formed is in solution that promotes a homogenous growth, leading to the formation of colloids. For all the different treatments of acid performed on the VGCFs, colloidal growth was observed at 20 h (and longer). All of the 4-h growth runs gave the least colloidal growth with the exception of the Type I acid treatment performed on the Pyrograph fibers from NASA, which have low hydroxyl content (see above). The best results were obtained by Type II acid treatment for both 4 and 8 h runs on the Pyrograph III VGCFs obtained from NASA as well as from MER (Fig. 4a and b). Interestingly the Type II acid treatment on Pyrograph III

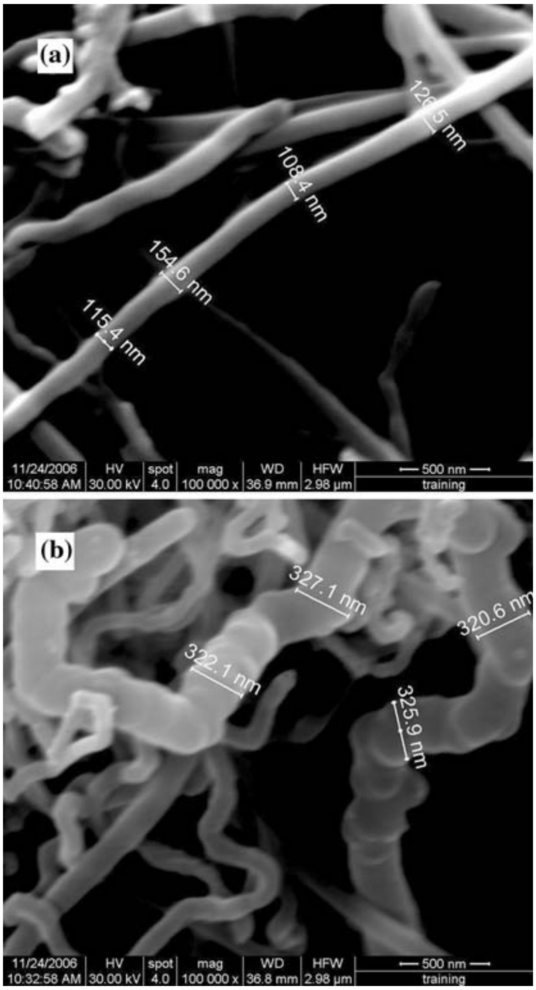

Fig. 5 SEM image of Type II treated VGCFs (Pyrograph III) (**a**) before and (**b**) after silica LPD for 4 h showing the presence of a 90–100 nm silica coating

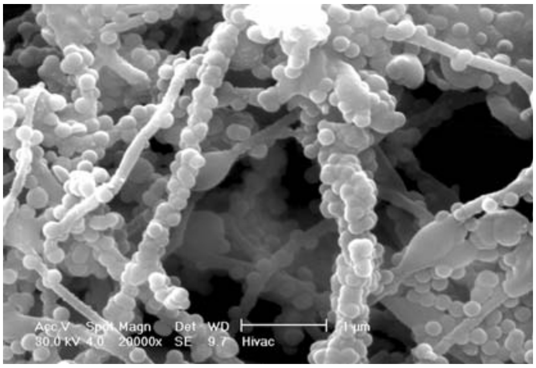

Fig. 6 SEM image of VGCFs (Pyrograph III) in DTAB coated with silica for 4 h, showing the presence of silica spheres resulting from the interaction of the silica LPD solutions with the DTAB micelles

VGCFs received from the Air Force gave a very colloidal growth for the 8 h run, despite the significant presence of hydroxyl groups.

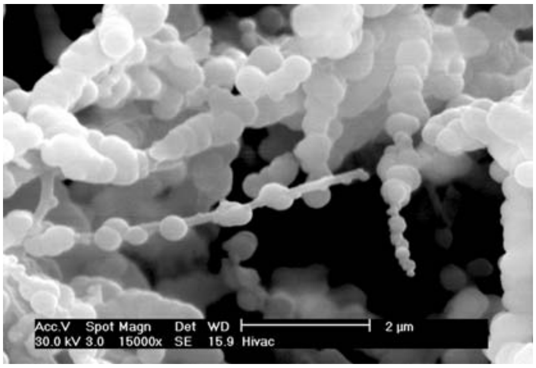

Fig. 7 SEM image of Type I treated VGCFs (Pyrograph III) coated with silica for 4 h

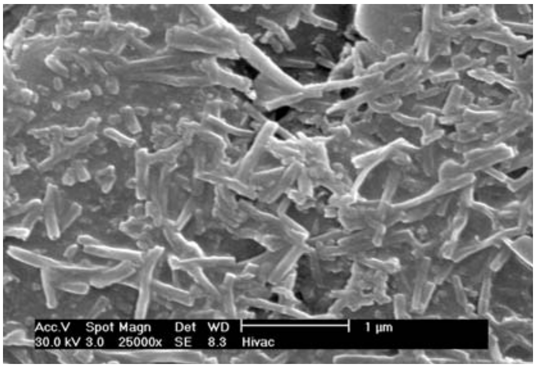

Fig. 8 SEM image of Type III acid treated VGCFs (Pyrograph III) coated with silica for 3 h

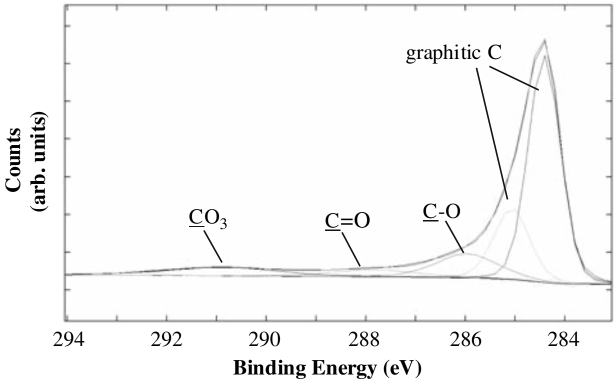

Fig. 9 High resolution C_{1s} XPS spectrum for Type II acid treated MER VGCFs showing the presence of different carbon species

Summary and conclusions

We have investigated three different acid treatments for the activation of VGCFs towards coating with silica via a LPD process. It was found that irrespective of the type of VGCF, heating a suspension of VGCFs in nitric acid to dryness (Type II) gave us the best results in terms of silica growth

Table 3 Percentage area of functional groups in C_{1s} spectra (%)

VGCF Sample	Treatment	Graphitic[a]	*C*–O[b]	*C*=O[c]	CO_3[d]
Pyrograph III (NASA)	n/a	90.21	2.82	4.60	2.37
Pyrograph III (NASA)	Type I	83.04	6.39	4.16	6.40
Pyrograph III (NASA)	Type II	76.99	11.02	6.5	5.48
Pyrograph III (Air Force)	n/a	80.91	9.85	4.94	4.3
Pyrograph III (Air Force)	Type II	70.75	15.23	9.92	4.1
Pyrograph III (Air Force)	Type III	65.14	15.04	15.22	4.6
MER corp.	n/a	78.61	8.55	5.42	7.43
MER corp.	Type I	79.22	10.26	3.29	7.23
MER corp.	Type II	75.5	12.84	5.56	6.38

[a] Graphitic carbon: 284.3–284.6 eV and 284.7–285.4 eV; error within 0.5 eV range

[b] Hydroxyl: 286.0–386.9 eV; error within 0.5 eV range

[c] Carbonyl: 287.8–288.7 eV; error within 0.5 eV range

[d] Carbonate: 289.1–290.8 eV and 291.0–292.2 eV; error within 0.5 eV range

around the VGCF. We also found that there is a correlation between the percent of hydroxyls present on the VGCF surface and the type of growth that occurs on the VGCF. Between the three acid treatments, Type II and Type III treatments gave a higher hydroxyl oxidation percent that Type I. Silica coating fibers treated using Type III treatment was highly soluble in EtOH, and hence difficult to wash off excess silica that may be present, making it difficult to see individual silica fibers.

Acknowledgements Financial support for this work was provided by NASA. Dr. Benji Maruyama (Wright Patterson Air Force Base, OH), Pasha Nickolaev, Olga Gorelik, Sivaram Arepalli and Leonard Yowell (NASA Johnson Space Center, TX) are acknowledged for donation of VGCFs and useful discussion.

References

1. Huges TV, Chambers CR (1889) US patent 405480
2. Yang Y, Liu X, Xu B, Li T (2006) Carbon 44:1661
3. Tibbetts GG, Beetz CP Jr (1987) J Phys D: Appl Phys 20:292
4. Lakshminarayanan PV, Toghiani H, Pittman CU Jr (2004) Carbon 42:2433
5. Oberlin A, Endo M, Koyama T (1976) J Cryst Growth 32:335
6. Wang Y, Viswanathan H, Audi AA, Sherwood PMA (1999) Chem Mater 12:1100
7. http://tpsx.arc.nasa.gov/index.html (08/16/06)
8. Marschall J, Milos FS (1998) J Thermodyn Heat Transfer 12:528
9. Clyne TW, Golosnoy IO, Tan JC, Markaki AE (2006) Phil Trans R Soc A 364:125
10. Rice RW (1998) Porosity of ceramics; Materials engineering 12; Marcel Dekker Inc., New York, NY, pp 315–368
11. Stewart DA, Leiser DB (1985) Ceram Eng Sci Proc 6:769
12. Whitsitt EA, Barron AR (2003) Nano Lett 3:775
13. Chanthamaly P, Arakawa T, Haneji N (1999) Jpn J Appl Phys, Part 1 38:5715
14. Huang C-J (2002) Jpn J Appl Phys, Part 1 41:4622
15. Colorado R Jr, Barron AR (2004) Chem Mater 16:2691
16. Whitsitt EA, Barron AR (2003) Chem Commun 9:1042
17. Anderson RE, Barron AR (2005) Main Group Chem 4:279
18. Whitsitt EA (2005) Ph.D. Thesis, Rice University, Houston, TX
19. Whitsitt EA, Moore VC, Smalley RE, Barron AR (2005) J Mater Chem 15:4678
20. Whitsitt EA, Barron AR (2005) J Colloid Interface Sci 287:318
21. Lee M-K, Shih C-M, Yang C-D (2003) Semicond Sci Technol 18:L45
22. Homma T, Katoh T, Yamada Y, Murao Y (1993) J Electrochem Soc 140/8:2410
23. Xie Y, Sherwood MAP (1990) Chem Mater 2:293
24. Moulder JF, Stickle WF, Sobol PE, Bomben KD (1995) In: Chastain J, Kings RC Jr (eds) Handbook of X-ray photoelectron spectroscopy. Physical Electronics Inc., Eden Prarie, MN, pp 40–41